

# Mathematical Methods in Machine Learning

Wojciech Czaja

UMD, Spring 2016



# Outline

## 1 Lecture 3: Role of Directionality Continued

# Recall the Fast Finite Shearlet Transform (FFST)

- Consider an  $M \times N$  image. Define  $j_0 := \lfloor \log_2 \max\{M, N\} \rfloor$ . We discretize the parameters as follows:

$$a_j := 2^{-2j} = \frac{1}{4^j}, \quad j = 0, \dots, j_0 - 1,$$

$$s_{j,k} := k2^{-j}, \quad -2^j \leq k \leq 2^j,$$

$$t_m := \left( \frac{m_1}{M}, \frac{m_2}{N} \right), \quad m_1 = 0, \dots, M-1, \quad m_2 = 0, \dots, N-1.$$

- Note that the shears vary from  $-1$  to  $1$ . To fill out the remaining directions, we also shear with respect to the  $y$ -axis.
- Shearlets whose supports overlap are “glued” together.
- The transform is computed through the  $2D$  FFT and iFFT.

# Fast Finite Shearlet Transform

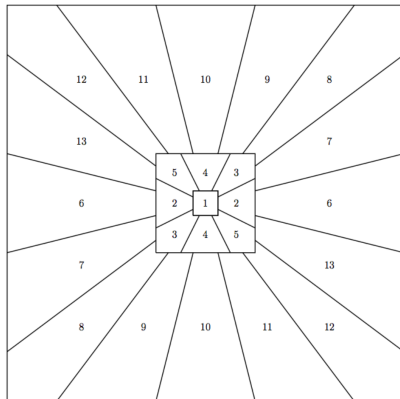


Figure : Frequency tiling for FFST.

S. Häuser and G. Steidl. *Fast finite shearlet transform: a tutorial*. arXiv:1202.1773. (2014).

# Additional Picture for FFST

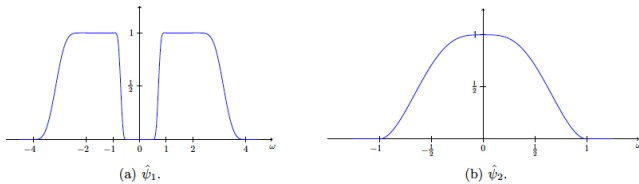
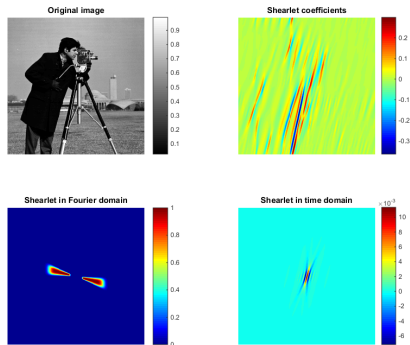


Figure :  $\hat{\psi}_1$  and  $\hat{\psi}_2$  for the FFST.

ibid.

# Fast Finite Shearlet Transform



**Figure :** Demonstration of output from the FFST on the cameraman image. The shearlet coefficients are from scale 3 (out of 4) in the direction of slope 4.

ibid

# How Well Can the FFST Resolve Directions?

We can prove that the direction of the shearlet coefficient of maximum magnitude determines the direction, at least in the ideal case.

## Theorem (with D. Weinberg, 2015)

Let  $f(x) = H_{y>rx}$  be a 2D Heaviside function and assume WLOG that  $|r| \leq 1$ . Fix a scale  $j$  and position  $m$ . Then the shearlet coefficient of the FFST  $\mathcal{SH}(f)(j, k, m)$  is only nonzero for at most two consecutive values of the shearing parameter  $k$ . The value of  $k$  that maximizes  $|\mathcal{SH}(f)(j, k, m)|$  satisfies

$$|s_{j,k} - r| < \frac{1}{2^j}.$$

Furthermore, for this  $k$ ,  $s_{j,k}$  is closest to  $r$  over all  $k$ .

D. Weinberg, Multiscale and Directional Representations of High-dimensional Information in Remotely Sensed Data, Ph.D. Thesis,

University of Maryland College Park, 2015

# Sketch of Proof

- We first show by direct computation that  $\int_{\mathbb{R}} \widehat{\psi}(-r\omega, \omega) d\omega = \int_{\mathbb{R}} \psi(x, rx) dx$  for all  $\psi \in \mathcal{S}(\mathbb{R}^2)$ ,  $r \in \mathbb{R}$ .
- Since  $\frac{\partial}{\partial y} H_{y>rx} = \delta_{y-rx}$ ,  $\widehat{H_{y>rx}} = \frac{1}{2\pi i \omega_2} \widehat{\delta_{y-rx}}$ .
- Using the above,  $\langle \widehat{\delta_{y-rx}}, \widehat{\psi} \rangle = \int_{\mathbb{R}} \widehat{\psi}(-r\omega, \omega) d\omega$ ,  $\widehat{\psi} \in C_c^\infty(\mathbb{R}^2)$ .
- We compute

$$\begin{aligned}
 \mathcal{SH}(f)(j, k, m) &= \langle f, \psi_{jkm} \rangle \\
 &= \langle \widehat{f}, \widehat{\psi}_{jkm} \rangle \\
 &= \int_{\mathbb{R}^2} \frac{1}{2\pi i \omega_2} \widehat{\delta_{y-rx}}(\omega_1, \omega_2) \widehat{\psi}_{jkm}(\omega_1, \omega_2) d\omega_1 d\omega_2 \\
 &= \frac{1}{2\pi i} \int_{\mathbb{R}} \frac{1}{\omega_2} \widehat{\psi}_{jkm}(-r\omega_2, \omega_2) d\omega_2.
 \end{aligned}$$



# Sketch of Proof

- By the way  $\hat{\psi}$  decomposes,

$$\hat{\psi}_{jkm}(-r\omega_2, \omega_2) = \hat{\psi}_1(4^{-j}\omega_2)\hat{\psi}_2(-2^j r + k) \exp(-2\pi i(-r\omega_2 m_1/M + \omega_2 m_2/N))$$

- Since  $k$  only appears in  $\hat{\psi}_2(-2^j r + k)$ , we examine that term separately.
- By assumption,  $\hat{\psi}_2$  is a positive, smooth function supported on  $[-1, 1]$  that is strictly increasing on  $[-1, 0]$  and decreasing on  $[0, 1]$ .
- Hence, to obtain a nonzero shearlet coefficient, we must have  $|-2^j r + k| < 1$  or  $|s_{j,k} - r| < 1/2^j$ .
- The shearlet slopes differ by  $1/2^j$ , so this can only occur at most twice.
- The coefficient is maximized when  $-2^j r + k$  is closest to 0, that is, when  $s_{j,k}$  is closest to  $r$ .

# Shearlets - a few results

- Shearlet multiresolution analysis theory and decomposition algorithm - G. Kutyniok and T. Sauer
- Shearlet approach to edge detection - S. Yi, D. Labate, G. Easley, and H. Krim
- Shearlet-based method to invert the Radon transform - F. Colonna, G. R. Easley, K. Guo, and D. Labate

All of the above results are in the setting of  $\mathbb{R}^2$ . But we are also interested in higher dimensional constructions.

# Translation-dilation-shearing group

- E. Cordero, F. DeMari, K. Nowak, and A. Tabacco introduced the following group interpretation of shearlets, by means of the **Translation-Dilation-Shearing Group**:

$$\left\{ A_{t,\ell,y} = \begin{pmatrix} t^{-1/2} S_{\ell/2} & 0 \\ t^{-1/2} B_y S_{\ell/2} & t^{1/2} (S_{-\ell/2}^t) \end{pmatrix} : t > 0, \ell \in \mathbb{R}, y \in \mathbb{R}^2 \right\},$$

where  $B_y = \begin{pmatrix} 0 & y_1 \\ y_1 & y_2 \end{pmatrix}$ ,  $y = (y_1, y_2)^t \in \mathbb{R}^2$ ,  $S_\ell = \begin{pmatrix} 1 & \ell \\ 0 & 1 \end{pmatrix}$ .

- Stems from attempts to characterize reproducing subgroups of  $\mathbb{R}^{2d} \rtimes \text{Sp}(2d, \mathbb{R})$ .
- We aim to generalize it to  $d \geq 2$ .

# Translation-dilation-shearing group in $\mathbb{R}^k$

- For  $k \geq 1$ , we define  $(\text{TDS})_k$  to be

$$\left\{ A_{t,\ell,y} = \begin{pmatrix} t^{-1/2} S_{\ell/2} & 0 \\ t^{-1/2} B_y S_{\ell/2} & t^{1/2} S_{-\ell/2}^t \end{pmatrix} : t > 0, \ell \in \mathbb{R}^{k-1}, y \in \mathbb{R}^k \right\}$$

- $y = (y_1, y_2, \dots, y_k)^t \in \mathbb{R}^k$

$$\bullet B_y = \begin{pmatrix} 0 & 0 & \dots & y_1 \\ 0 & 0 & \dots & y_2 \\ \vdots & \vdots & \ddots & \vdots \\ y_1 & y_2 & \dots & y_k \end{pmatrix}, S_\ell = \begin{pmatrix} 1 & 0 & \dots & 0 & \ell_1 \\ 0 & 1 & \dots & 0 & \ell_2 \\ \vdots & \vdots & \ddots & \vdots & \\ 0 & 0 & \dots & 1 & \ell_{k-1} \\ 0 & 0 & \dots & 0 & 1 \end{pmatrix}$$

# Translation-dilation-shearing group in $\mathbb{R}^k$

- The *symplectic group*  $\text{Sp}(d, \mathbb{R})$  is the subgroup of  $2d \times 2d$  matrices  $g \in \text{M}(2d, \mathbb{R})$  which satisfy  $g^t \mathcal{J} g = \mathcal{J}$ , where

$$\mathcal{J} = \begin{pmatrix} 0 & I_d \\ -I_d & 0 \end{pmatrix}.$$

## Theorem (with E. King)

For any  $k \geq 1$ ,  $(\text{TDS})_k$  is a Lie subgroup of  $\text{Sp}(k, \mathbb{R})$  of dimension  $2k$ . The left Haar measures, up to normalization, of  $(\text{TDS})_k$  are  $d\tau = \frac{dt}{t^2} dy$  for  $k = 1$  and  $d\tau = \frac{dt}{t^{k+1}} dy d\ell$  for  $k > 1$ , where  $dt$ ,  $dy$  and  $d\ell$  are the Lebesgue measures over  $\mathbb{R}^+$ ,  $\mathbb{R}^k$  and  $\mathbb{R}^{k-1}$ , respectively.

E. J. King, Wavelet and frame theory: frame bound gaps, generalized shearlets, Grassmannian fusion frames, and p-adic wavelets, Ph.D. Thesis, University of Maryland College Park, 2009

W. Czaja, E. King, Isotropic shearlet analogs for  $L^2(\mathbb{R}^k)$  and localization operators, Numerical Functional Analysis and Optimization 33 (2012), no. 7-9, pp. 872–905

W. Czaja, E. King, Shearlet analogs of  $L^2(\mathbb{R}^d)$ , Math. Nachr. 287 (2014), no. 89, pp. 903–916

# Reproducing functions

- We are interested in reproducing formulas, which hold for all  $f \in L^2(\mathbb{R}^d)$ ,

$$f = \int_H \langle f, \mu_e(h)\phi \rangle \mu_e(h)\phi dh,$$

where  $H$  is a Lie subgroup of a particular Lie group,  $\mu_e$  is a representation of that group,  $\phi$  is a suitable window in  $L^2(\mathbb{R}^d)$ , and the equality is interpreted weakly.

- Define the metaplectic representation:

$$\mu(A_{t,\ell,y})f(x) = t^{k/4} e^{-i\pi\langle B_y x, x \rangle} f(t^{1/2} S_{-\ell/2} x).$$

- 

$$A_{t,\ell,y} = \begin{pmatrix} t^{-1/2} S_{\ell/2} & 0 \\ 0 & t^{1/2} (S_{-\ell/2}^t) \end{pmatrix} \begin{pmatrix} I & 0 \\ t^{-1} (S_{\ell/2}^t) B_y S_{\ell/2} & I \end{pmatrix}.$$

# Calderón admissibility condition

## Theorem (Calderón formula, with E. King)

The following equality holds

$$\|f\|_{L^2(\mathbb{R}^k)}^2 = \int_{(TDS)_k} |\langle f, \mu(A_{t,\ell,y})\phi \rangle|^2 \frac{dt}{t^{k+1}} dy d\ell$$

for all  $f \in L^2(\mathbb{R}^k)$ , if and only if

$$2^{-k} = \int_{\mathbb{R}_+^k} |\phi(y)|^2 \frac{dy}{y_k^{2k}} = \int_{\mathbb{R}_+^k} |\phi(-y)|^2 \frac{dy}{y_k^{2k}} \quad (1)$$

$$0 = \int_{\mathbb{R}_+^k} \bar{\phi}(y)\phi(-y) \frac{dy}{y_k^{2k}}. \quad (2)$$

- The case  $k = 1$  was proven by DeMari and Nowak.

# Building reproducing functions

## Theorem (with E. King)

Let  $f : \mathbb{R} \rightarrow \mathbb{R}$  be supported in some interval  $[0, b]$ ,  $b > 0$  and satisfy  $\int f^2(x)dx = \frac{1}{4}$ . For  $a > 0$ , define

$$\phi(x) = x(f(x-a) - f(-x+a+2b)) + f(x+a+b) + f(-x-a-b).$$

Then  $\phi$  is a reproducing function for  $(\text{TDS})_1$ .

- $f = \mathbb{1}_{[0, \frac{1}{4}]}$
- $f = \frac{1}{\sqrt{\pi}} \cos \cdot \mathbb{1}_{[0, \frac{\pi}{2}]}$
- $f \in C_c^\infty(\mathbb{R})$  has support in  $[0, b]$  and is scaled so that  $\int f^2 = \frac{1}{4}$ , then the resulting  $\phi$  will also lie in  $C_c^\infty$



# Uniqueness of generalization

- Dahlke, Steidl, and Teschke introduced another  $k$ -dimensional shearlet transform.
- This construction does not yield a reproducing subgroup of  $Sp(k, \mathbb{R})$ .
- The only pseudo-TDS collection which is a reproducing subgroup of  $Sp(k, \mathbb{R})$  and has a representation onto the operators  $T_y D_{t^{-1}(S'_t)}$  is  $(TDS)_k$ .

# Shearlets are not perfect

- Shearlet algorithms result in frames with high redundancy.
- There does not exist any compactly supported MRA shearlet with a desirable level of regularity (Houska, 2009), e.g., Hölder continuous in  $e_2$  with exponent  $\beta > 0.5$ .
- Most common implementations of shearlets involve separable generating functions..

# Composite Dilation Wavelets

- We return to the origin of wavelets: translations and dilations.
- Shearlets descend from the idea of composite wavelets as introduced by Guido Weiss.
- For any  $c \in GL_n(\mathbb{R})$  we define the dilation operator  $D_c : L^2(\mathbb{R}^n) \rightarrow L^2(\mathbb{R}^n)$  as  $D_c f(x) = |\det c|^{-1/2} f(c^{-1}x)$ .
- Let  $A, B \subset GL_n(\mathbb{R})$  and  $\mathcal{L} \subset \mathbb{R}^n$  be a full rank lattice, then the set  $\{\psi^1, \dots, \psi^L\} \subset L^2(\mathbb{R}^n)$  forms a *Composite Dilation Wavelet (CDW)* system if the collection

$$\mathcal{A}_{AB\mathcal{L}}(\psi) = \{D_a D_b T_k \psi^i : a \in A, b \in B, k \in \mathcal{L}, 1 \leq i \leq L\}$$

forms a normalized tight frame.

# Composite Dilation Wavelets

- Under the assumption that  $B$  is a finite group with  $B(\mathcal{L}) \subset \mathcal{L}$  and  $|\det b| = 1$ , for  $b \in B$ , Manning (2012) proposed to group the dilations  $B$  and the lattice  $\mathcal{L}$  together into a single group of shifts  $\Gamma = B\mathcal{L}$ .

B. Maning, Composite Multiresolution Analysis Wavelets, Ph.D. Thesis, Washington University in St. Louis, 2012

- For any  $\gamma \in \Gamma$ , we define the shift operator  $L_\gamma : L^2(\mathbb{R}^n) \rightarrow L^2(\mathbb{R}^n)$  as  $L_\gamma f(x) = f(\gamma^{-1}(x))$ .
- Given  $a \in GL_n(\mathbb{R})$ , the set  $\{\psi^1, \dots, \psi^L\}$  forms a CDW if the system

$$\mathcal{A}_{a\Gamma}(\psi) = \{D_{a^j} L_\gamma \psi^i : j \in \mathbb{Z}, \gamma \in \Gamma, 1 \leq i \leq L\}$$

forms a tight frame.

- CDW are usual wavelets except the commutative group of translates  $\mathbb{Z}^n$  is replaced with the non-commutative group of shifts  $\Gamma$ .

# Composite Dilation Wavelets

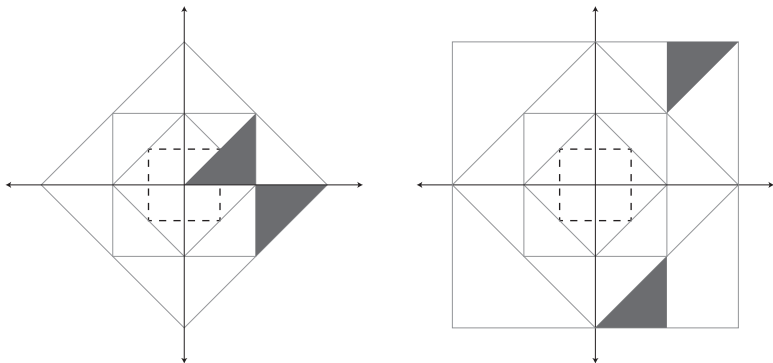


**Figure :** Example of a composite dilation wavelet. The picture on the left is the Fourier transform of the scaling function. The picture on the right is the Fourier transform of the wavelet.

# Variational methods with directional multiscale representations

- Ginzburg-Landau energy functionals have been used by A. Bertozzi and her collaborators in a number of image processing applications that involve variational techniques.

J. Dobrosotskaya and A. Bertozzi, "Analysis of the wavelet Ginzburg-Landau energy in image applications with edges," SIAM J. Imaging Sci., 2013, Vol. 6 (1), pp. 698–729.

- Wavelet-modified GL energies reduce blurring effects of the TV functionals, increase robustness, and sharpen edges.
- Isotropic wavelets are unable to take advantage of directional content. Anisotropy of wavelet bases and wavelet generator functions leads to biased analysis of singularities along different directions.

# Shearlet Ginzburg-Landau energy

- Let

$$\psi_{i,j,t} = 2^{3i/2} \psi(S_1^j A_2^i x - t),$$

for  $x \in \mathbb{R}^2$  and  $\hat{\psi}(\xi) = \hat{\psi}_1(\xi_1) \hat{\psi}_2(\xi_2/\xi_1)$ .

- Shearlet Besov seminorm is

$$\|u\|_S^2 = \sum_{i=0}^{\infty} 2^{2i} \sum_{j \in \mathbb{Z}} \int (|\langle u, \psi_{i,j,t} \rangle|^2 + |\langle u^*, \psi_{i,j,t} \rangle|^2) dt,$$

where  $u^*(x, y) = u(y, x)$ .

- Shearlet Ginzburg-Landau energy is

$$SGL_{\alpha}(u) = \frac{\alpha}{2} \|u\|_S^2 + \frac{1}{4\alpha} \int ((u^2(x) - 1)^2) dx.$$

# Composite Wavelet Ginzburg-Landau energy

- Let

$$\psi_{i,\gamma} = D_{a^{-i}} L_{\gamma} \psi,$$

for  $i \in \mathbb{Z}$  and  $\gamma \in \Gamma$ .

- Composite Wavelet Besov seminorm is

$$\|u\|_{CW}^2 = \sum_{i=0}^{\infty} |\det a|^i \sum_{\gamma \in \Gamma} |\langle u, \psi_{i,\gamma} \rangle|^2.$$

- Composite Wavelet Ginzburg-Landau energy is

$$CWGL_{\alpha}(u) = \frac{\alpha}{2} \|u\|_{CW}^2 + \frac{1}{4\alpha} \int ((u^2(x) - 1)^2) dx.$$



# Applications to data recovery

- In many imaging applications variational methods are based on minimizing an energy consisting of two parts: regularizing and forcing terms.
- DGL energy (D = S or CW) plays the role of a regularizer, while the forcing term is expressed as the  $L_2$  norm between the minimizer  $u$  and the known image  $f$  on the known domain:

$$E(u) = DGL(u) + \frac{\mu}{2} \|u - f\|_{L^2(\Omega)}^2.$$

- We recover the complete image as the minimizer of the modified DGL functional.

# Applications to data recovery

- The minimizer is a stable state solution of the respective gradient descent equation:

$$u_t = \alpha \Delta_D u - \frac{1}{\epsilon} W'(u) - \mu \chi_\Omega (u - f)$$

Here  $\chi_\Omega$  is the characteristic function of the known domain,  $W(x) = (x^2 - 1)^2$ , and

$$\Delta_{CW} u = - \sum_{i=0}^{\infty} |\det a|^i \sum_{\gamma \in \Gamma} \langle u, \psi_{i,\gamma} \rangle \psi_{i,\gamma},$$

or

$$\Delta_S(u) = - \sum_{i=0}^{\infty} 2^{2i} u_i - \sum_{i=0}^{\infty} 2^{2i} ((u^*)_i)^*.$$

# Shearlet inpainting

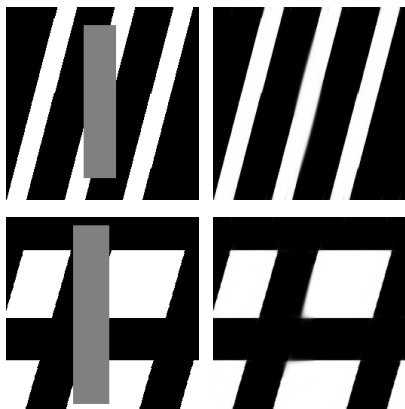


**Figure :** Results of anisotropic shearlet inpainting which preserves the directional distribution of the input data, as an illustration of the need to know the local and global directions in image processing.

W. Czaja, J. Dobrosotskaya, B. Manning, Shearlet representations for reconstruction of missing data, Proc. SPIE Vol. 8750 (2013), no. 8750-2

# Composite Dilation Wavelet Inpainting

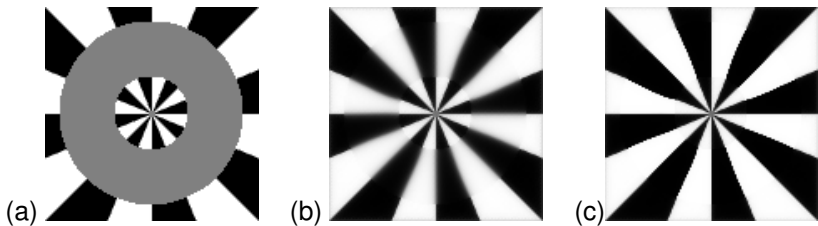


**Figure :** (a) Original image with gray area missing, (b) image reconstructed via minimizing CWGL after 100 iterations,  $\epsilon = 1/24$ ,  $\mu = 1600$ ; (c) post-processed images (b)

# Composite Dilation Wavelets vs Shearlets

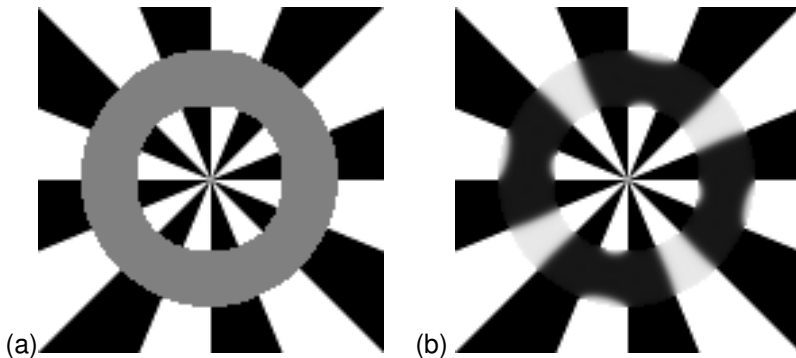


**Figure :** (a) Original image with gray area missing, (b) Shearlet inpainting does not show the required anisotropy, post-processing does not help

# Composite Dilation Wavelets may fail too

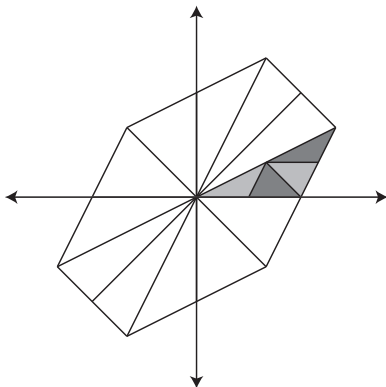


**Figure :** Another example of a composite dilation wavelet. The figure above describes the Haar scaling function and wavelet for the twelve element group  $B$ . The scaling function is supported and constant on both the light and dark shaded areas. There are four wavelet functions. Each wavelet function is supported on both the light and dark shaded areas and is constant on each

# Composite Dilation Wavelets may fail too

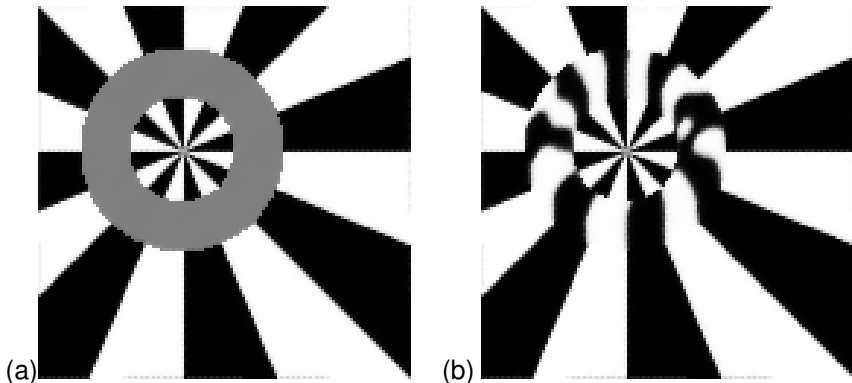


**Figure :** (a) Original image with a missing annulus is shown in gray, (b) the output of the inpainting simulation fails to reproduce our earlier results.

# Applications to superresolution

- Jointly with researchers from NGA, we exploited applications of directional methods for image super-resolution.

E. H. Bosch, et al., "Multiscale and multidirectional tight frames for image analysis," Proc. SPIE, Vol. 8750, 2013.



(a) Original Image



(b) Bicubic Interpolation



(c) Tight Frame Superresolution

**Figure :** Image taken from the MUUFL HSI-LIDAR dataset, courtesy of P. Gader (UFL) and A. Zare (UM). Spatial subset of a false-RGB combination comparing directional tight frame scheme to bicubic interpolation for doubling



# Summary and Conclusions

- We have covered some of the multiscale directional representations systems in use today.
- These systems come equipped with good approximation properties and have fast implementations.
- The difficulties arise in higher dimensions, where the computational complexity increases.
- Additionally, for more complex data structures, the a priori notion of direction may not be well defined.
- Finally, determining the set of directions without the reference to specific data is limiting. Next, we shall take a look at data dependent representations.